Magnon Raman spectroscopy and in-plane dielectric response in $BiFeO_3$: Relation to the Polomska transition

Ashok Kumar,[1,2,*] J. F. Scott,[1,3,†] and R. S. Katiyar[1,‡]

[1]*Department of Physics and Institute for Functional Nanomaterials, University of Puerto Rico, San Juan, Puerto Rico 00936-8377, USA*

[2]*Materials Physics and Engineering Division, National Physical Laboratory, Delhi 110012, India*

[3]*Department of Physics, Cavendish Laboratory, Cambridge University, Cambridge CB3 OHE, United Kingdom*

(Received 5 February 2012; revised manuscript received 1 May 2012; published 12 June 2012)

We report strong dielectric loss anomalies near 450 K in bismuth ferrite, together with anomalous magnon damping, and suggest that since this temperature is coincident with the mysterious "Polomska transition" [M. Polomska *et al*., Phys. Status Solidi A **23**, 567 (1974)] at 458 ± 5 K, this may indicate a surface phase transition. In bismuth ferrite thin films the cycloidal spiral spin structure is suppressed, and as a result the spin-wave magnon branches of long wavelength are reduced from a dozen to one, at $\omega = 19.2$ cm^{-1} ($T = 4$ K). This spin wave has not been measured previously in thin-film bismuth ferrite above room temperature, but in the present work we show via Raman spectroscopy that it is an underdamped propagating wave until 455 K. The data show that $\omega(T)$ follows an $S = 5/2$ Brillouin function, and hence its Fe^{+3} ions are in the high-spin 5/2 state and not the low-spin $S = 1/2$ state. The surface spin wave cannot be measured as a propagating wave above the Polomska transition at 458 K.

DOI: 10.1103/PhysRevB.85.224410 PACS number(s): 75.85.+t, 75.30.Ds, 77.22.−d, 77.84.−s

The production of high-quality thin films of bismuth ferrite has opened up the possibility of making room-temperature devices that rely on spin-wave propagation. In 2008 the study of spin waves via magnon Raman spectroscopy began,[1–5] and more recently a review was published on its device applications.[6] Foremost among the potential thin-film device applications are THz emitters,[7–9] and for the majority of devices (including electric-field tunable magnetic devices) the existence of room-temperature spin waves (magnons) that are propagating modes (as opposed to overdamped or diffusive modes) is important.[10–12]

Here we report propagating spin waves in thin-film $BiFeO_3$ (BFO) up to 450 K. Although in bulk there are numerous magnon branches at long wavelength that scatter light in the Raman effect (due to the cycloidal spin structure), in thin films this cycloid is suppressed and there is only a single magnon branch in the Raman spectra. Loudon and Fleury[13,14] provided the basic theory of magnon spectroscopy and damping. In general, systems with Fe or Co ions can exhibit unquenched orbital angular momentum; but despite the fact that they therefore are not pure spin systems, their temperature dependence and damping are not very different from those in pure spin systems such as Mn compounds.[15] Low-energy spin waves are observed in several ferro/antiferromagnetic systems and well explained with a phenomenological theory.[16–19] Here we report the temperature-dependent softening of spin waves, their suppression in thin-film form, correlation with a magnetic transition temperature, and dielectric loss. Softening of spin waves follows a modified Brillouin function with $S = 5/2$ [all Brillouin functions are mean field with critical susceptibility exponent beta ($\beta = 1/2$)].

Prepatterned platinum interdigital electrodes were procured from NASA Glenn Research Center's electronics division having dimensions 1900 μm (length), 15 μm (interdigital spacing), and 150 ± 25 nm (height) with 45 parallel capacitors in series on sapphire substrates. We used 20 polycrystalline BFO specimens of thicknesses from 100 to 200 nm. This is in the bulk limit for magnetic properties ("thin" for magnon properties is a few lattice constants). Most of these specimens show similar magnetic and in-plane dielectric properties. Figures 1(a), 1(b), and 1(c) show the cartoon of spin waves, their suppression to a spin arrangement similar to that in conventional two-sublattice antiferromagnetic systems, and the in-plane view of the BFO thin films on the prepatterned interdigital electrodes. The details of crystal phase formations, surface morphology, impurities, and electrical testing equipment and parameters were presented in previous reports.[1,5] BFO thin films were grown utilizing an excimer laser (KrF, 248 nm) with a laser energy density of 1.5 J/cm^2, laser repetition rate of 10 Hz, substrate temperature 650 °C, and oxygen pressure at 80 mTorr. Micro-Raman spectra were recorded in the backscattering geometry using 514.5 nm monochromatic radiations over a wide range of temperature utilizing low-temperature cryostage from Linkam.

Figure 2 demonstrates the variation of low-energy spin waves at various temperatures. Only one spin wave was observed in the low-frequency Raman spectra that is sharp and can be clearly seen beyond the baseline noise background. These low-energy spin waves are underdamped until 450 K with a narrow magnon peak. Spin waves shift to lower frequencies with increasing temperature; due to stray light and spectrometer characteristics, our experimental limitation was to observe the Raman spectra only above 10 cm^{-1}.

Figure 3 shows the scaling behavior of magnon frequencies $\omega(T)$ versus temperature in one of our films. Note that the frequency data $\omega(T)$ satisfy a mean-field $S = 5/2$ high-spin Brillouin function much better than a low-spin $S = 1/2$ Brillouin function. It is already known from a series of elegant papers by Gavriliuk *et al*. in Moscow[20–23] that the Fe^{+3} ions in the insulating state of bismuth ferrite have $S = 5/2$, whereas the metallic state has $S = 1/2$, so this only confirms previously established conclusions. However, this is the first time such conclusions have been inferred purely from Raman

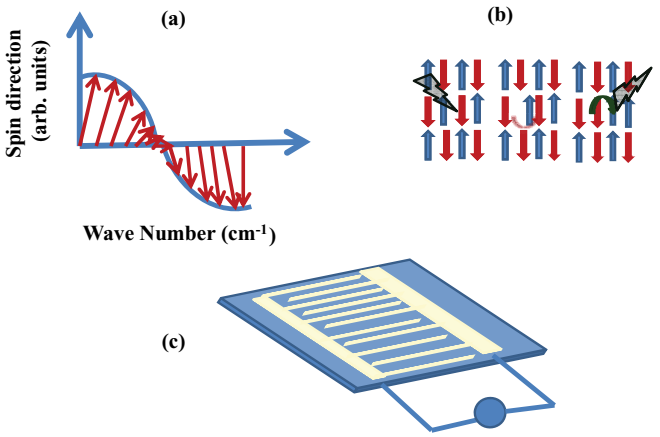

FIG. 1. (Color online) Schematic diagram and cartoon of the spin waves, spin-wave generation by antiferromagnetic materials, and the in-plane view of the BFO thin films. (a) Spin-wave propagation in the BFO single crystal. (b) The mechanism for the suppression of spin waves from several frequencies to a single frequency is illustrated for an antiferromagnet. (c) Schematic diagram of the in-plane view of the BFO thin films grown on the prepatterned interdigited electrode.

magnon spectroscopy in any material, so that it provides a nice pedagogical example.

BFO thin film shows only one spin-wave excitation whereas its single-crystal form exhibits several spin excitations. We employed a molecular field theory for this magnon frequency based on a macroscopic model with $H_A = |\lambda M_1|$ and $H_E = |\mu M_2|$, where H_A and H_E indicate anisotropy field and exchange field, respectively, where M_1 and M_2 are the magnetic moments progressed due to anisotropy and exchange

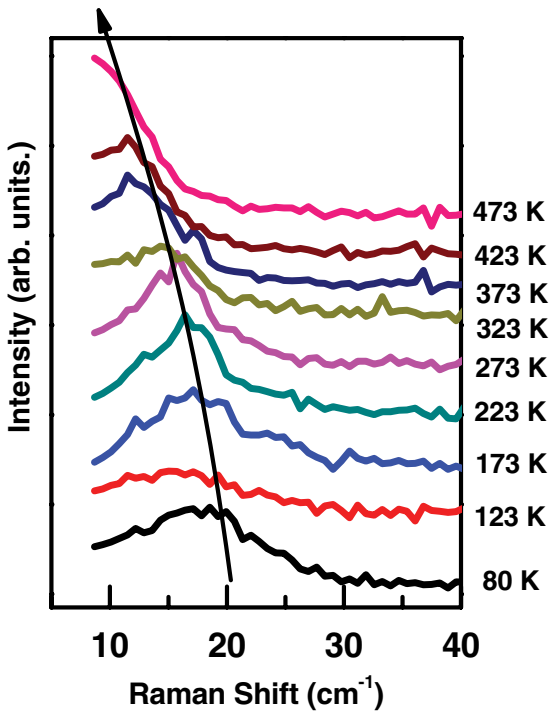

FIG. 2. (Color online) Low-lying spin waves probed by Raman spectroscopy at various temperatures (80 K to 473 K). The magnon frequency shifted to lower frequencies with increasing temperature.

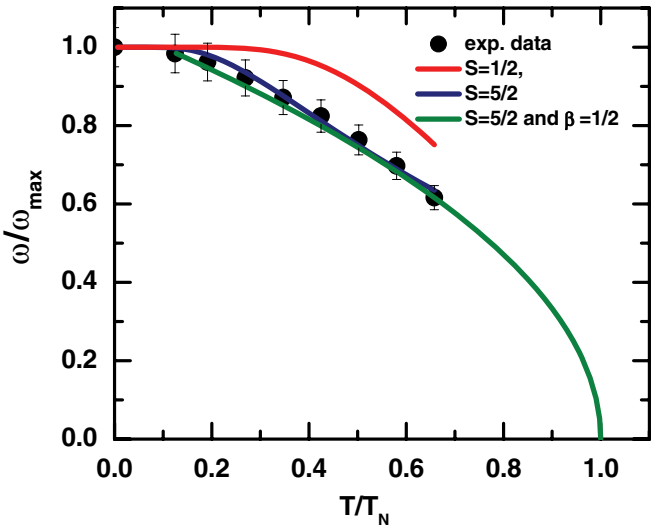

FIG. 3. (Color online) Magnon frequency versus temperature in bismuth ferrite thin films. Experimental values of spin-wave frequency are presented as solid dots with experimental error bars. The curves are least-squares fits to $S = 1/2$ (low spin) (red solid line) and $S = 5/2$ (high spin) (blue solid line) for the magnon frequency for the Fe^{+3} ions utilizing the low-temperature spin theory [Eqs. (1) and (8)]. The theoretical fitting of the complete temperature range from the Néel temperature to absolute zero is shown by the third curve (green solid line), which fitted well the modified mean molecular field model (the label $\beta = 1/2$ emphasizes the mean-field behavior). Note that magnon frequency theoretically is not quite proportional to the magnetization $M(T)$.

field based magnetic excitations.[16] λ and μ are the coefficient of proportionality between the anisotropy field and exchange field and their saturation magnetization, respectively; it can be also be utilized to get exchange energy of the system.

The solution of Bloch equations provides the low lying magnon frequency:

$$\omega_m = \gamma\left(H_A^2 + 2H_A H_E\right)^{1/2}, \qquad \gamma = ge/2mc, \quad S = 5/2, \quad g = 2, \tag{1}$$

where γ is the gyromagnetic ratio of Fe^{3+} ions, m is the electronic mass, g is the g factor, c is the speed of light, and e is the electronic charge.

In the framework of molecular field theory the net magnetization is the superposition of two interpenetrating magnetizations M_1 and M_2 preferentially parallel and antiparallel to magnetic field. It is assumed that the H_A and H_E are the proportional to the saturation values of M_1 and M_2 given by

$$M_s = (2g\mu_B S/a^3)B_s(y), \tag{2}$$

where M_s is the contribution coming from adding M_1 and M_2 of a two-sublattice antiferromagnet, μ_B is the Bohr magneton, a is the lattice constant, and $B_S(y)$ is the Brillouin function. Here we used the spin-labeled Brillouin function $B_S(y)$ instead of the Brillouin function $B_J(y)$ with total angular momentum quantum number J, since for the high-spin $S = 5/2$ state $L = 0$ and so $J = S$. For the low-spin $S = 1/2$ state L is not exactly zero but is heavily quenched by the noncentric rhombohedral

crystal field, so J is nearly S.

$$B_S(y) = \frac{2S+1}{2S}\coth\left(\frac{(2S+1)y}{2S}\right) - \frac{1}{2S}\coth\left(\frac{y}{2S}\right),$$

where the argument y is a real variable and S is a positive half-integer; in general y represents the ratio of Zeeman energy of magnetic moment under external magnetic field to that of the thermal energy k_BT, where k_B is the Boltzmann constant. For $y = \frac{\mu_B}{k_BT} \ll 1$, $\coth y = \frac{1}{y} + \frac{y}{3} - \frac{y^3}{45}$,

$$y = \frac{g\mu_B S}{\kappa_B T}(H_A + H_E) \equiv \frac{g\mu_B S}{\kappa_B T}(\lambda + \mu)M_S, \quad (3)$$

$$k_B T_N = (2/3a^3)g^2{\mu_B}^2 S(S+1)(\lambda + \mu). \quad (4)$$

Equation (2) is solved with assumption that ω_m is proportional to M_s and equal to 19.2 cm^{-1} at $T = 0$ K and $T_N \sim$631.5 K (power-law fitting of experimental data). These equations are for a two-sublattice antiferromagnet and differ by factors of two from the one-lattice ferromagnet equation in elementary texts.[18] Solving Eq. (2) gives the curves in Fig. 3. We have utilized Eqs. (3) and (4) to solve Eq. (2) and the Brillouin function. This theoretical model has been used to see the softening of the low-lying magnon branch for most antiferromagnetic systems. Our experimental data fitted well with the theory for S very near to spin 5/2. Darby has obtained the numerical values and the equations for the spontaneous magnetization and their softening behavior for magnetic system with different spin behavior.[17]

Near the Néel temperature $T/T_N \to 1$ ($y \ll 1$), the Brillouin function and scaled magnetization will follow the equations

$$B_S(y) = \frac{(2S+1)^2 - 1}{(2S)^2}\frac{y}{3} - \frac{(2S+1)^4 - 1}{(2S)^4}\frac{y^3}{45} + \ldots, \quad (5)$$

$$\left(\frac{M}{M_0}\right)^2 = \frac{10}{3}\frac{(S+1)^2}{(S+1)^2 + S^2}\left(1 - \frac{T}{T_N}\right) + \ldots, \quad (6)$$

whereas M and M_0 are the magnetic moment at variable temperature T and near absolute zero (0 K). The Brillouin function and scaled magnetization can be obtained from Eqs. (7) and (8):

$$B_S(y) = 1 - \frac{1}{S}\exp\left(-\frac{y}{S}\right) + \left(\frac{2S+1}{S}\right) \times \exp\left(\frac{-(2S+1)y}{S}\right) + \ldots, \quad (7)$$

$$\left(\frac{M}{M_0}\right) = 1 - \frac{1}{S}\exp\left(-\frac{3}{S+1}\frac{T_N}{T}\right) + \ldots \quad (8)$$

Here for the high-spin $S = 5/2$ state $L = 0$ and so $J = S$. For the low-spin $S = 1/2$ state L is not exactly zero but is heavily quenched by the noncentric rhombohedral crystal field, so J is nearly S. We use the quenched orbital angular momentum in what follows. Equations (6) and (8) together provide values of magnetization and the Brillouin function near low temperature (absolute zero K) and the Néel point, respectively. Utilizing both equations one can sketch the complete range of magnetization versus temperature scaling behavior. Note that the curves must intersect $T = 0$ horizontally due to the third law of thermodynamics.

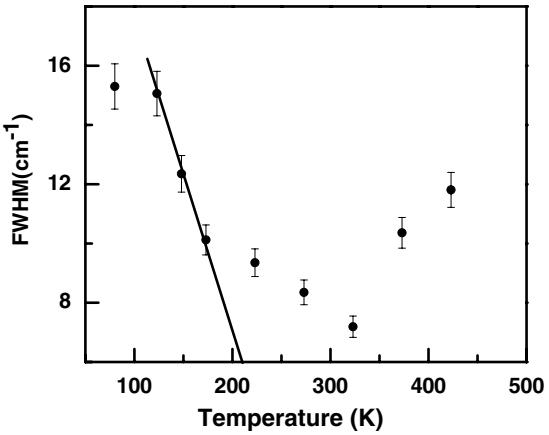

FIG. 4. Temperature-dependent linewidth of magnon frequency showing a rapid decrease in linewidth until 210 K, with further slow decrease between 210 K and room temperature. In the higher temperatures (above room temperature) it shows increase in linewidth with increasing temperature.

It is worth mentioning that magnon frequency is directly proportional to magnetization with a factor that also involves the spin factor: $\omega_m = \gamma M^b$, where $b = 1$,

$$g_J = 1 + \frac{S(S+1) + J(J+1) - L(L+1)}{2J(J+1)},$$

$S = 5/2$, $g = 2$, for the high-spin state. But for the low spin the value of $1.5 < g < 2$, and we consider $g = 1.5$ in our fitting parameters. We have utilized the low-temperature spin-wave theory since experimental data only reached up to 70% of the Néel temperature T_N.

The scaling behavior follows well $S = 5/2$ for both low temperature and near the Néel temperature. $S = 1/2$ is a very poor fit to the experimental data. It is worth mentioning that our spin-wave softening matches quantitatively with the recent observation of the magnon softening probed by terahertz spectroscopic studies.[9] The magnon damping is of special interest; temperature-dependent linewidths of the magnons are presented in Fig. 4. As noted above, it is modest until about 150 K above ambient. It decreases linearly till 210 K (± 5) with further decrease with a smaller slope to a minimum (unexplained but mirrored in the dielectric loss and probably due to surface condensation including water/ice) around 270–300 K. We find that it is no longer measurable as a propagating wave above 450 $\pm$ 10 K; it has broadened dramatically and is overdamped. It is not unusual for magnons to become overdamped at temperatures of order 70%–80% T_N, but in the case of bismuth ferrite, this might not be entirely coincidental, since a yet enigmatic phase transition has been reported[24,25] in some specimens at 458 $\pm$ 5 K. If this is indeed the temperatures of a subtle structural phase transformation (surface[26] or bulk), then one might expect anomalous damping at nearby temperatures. In order to test this coincidence, we present in the final section a complementary study of in-plane dielectric loss, which confirms the strong connection to the Polomska transition. These show an anomalous decrease in the spin linewidth near the so-called spin reorientation transition (210 K) but with nonmonotonic behavior, increasing at higher temperatures. The detailed phenomena near the

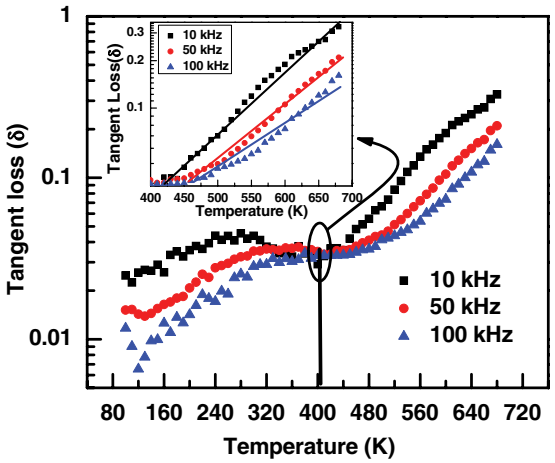

FIG. 5. (Color online) In-plane loss tangent (at 10 to 100 kHz) of BFO thin films showing broad maximum near the onset of the magnetic phase transition temperature and sharp increase above the Polomska transition near 458 K. Inset shows linear relation of tangent loss above the onset of the Polomska transition.

presumed magnetic transition at about 210 K are discussed in earlier reports.[1–5] It is interesting that the in-plane loss tangent of BFO is very small up to 450 K (only 1%–2% dielectric loss was observed as can be seen from Fig. 5). Figure 5 (inset) shows almost linear behavior in dielectric loss spectra near 450 K at 10 kHz, 50 kHz, and 100 kHz frequencies. As mentioned above, the broad low dielectric loss peak from about 270–300 K is probably surface condensation from the atmosphere. A reproducible broad loss peak ("hump") was also observed near the 210 K magnetic transition for a wide range of frequency. The detailed in-plane dielectric properties of BFO will be presented elsewhere. It is presumably not a coincidence that the dielectric loss also starts increasing above 450 K where the magnon branch disappears as a propagating mode.

In summary, we report high-temperature spin-wave propagation and temperature dependence in BFO thin films. The spin waves remain underdamped until 450 K with a sharp magnon peak. Propagating spin waves were not observed at elevated temperatures. The magnon frequency follows an $S = 5/2$ Brillouin function and hence its Fe^{+3} ions are in the high-spin 5/2 state. The linewidth demonstrates an anomalous decrease near the magnetic transition temperature but increases strongly at higher temperatures. A dielectric peak less broad in temperature was also observed near the onset of the 210 K magnetic transition over a wide temperature range, and not coincidentally, it again starts increasing rapidly above the 450 K Polomska transition, at which the spin waves no longer are observed as propagating waves. Above the Polomska transition the dielectric loss at 10 kHz increases linearly with temperature up until 800 K; measurements from 10 kHz to 100 kHz were very similar. This work implies that the heretofore mysterious Polomska anomaly is real and is a surface phase transition, similar to that 90 K higher at 548 K studied very recently by Marti *et al.*[26]

This work was supported in part by DOE-DE-FG02-08ER46526 and IFN-NSF-RII 07-01-25 grants.

*ashok553@gmail.com
†jfs32@hermes.cam.ac.uk
‡rkatiyar@uprrp.edu

[1] A. Kumar, N. M. Murari, and R. S. Katiyar, Appl. Phys. Lett. **92**, 152907 (2008).
[2] M. Cazayous, Y. Gallais, A. Sacuto, R. de Sousa, D. Lebeugle, and D. Colson, Phys. Rev. Lett. **101**, 037601 (2008).
[3] P. Rovillain, M. Cazayous, Y. Gallais, A. Sacuto, R. P. S. M. Lobo, D. Lebeugle, and D. Colson, Phys. Rev. B **79**, 180411 (2009).
[4] M. K. Singh, R. S. Katiyar, and J. F. Scott, J. Phys.: Condens. Matter **20**, 252203 (2008).
[5] A. Kumar, J. F. Scott, and R. S. Katiyar, Appl. Phys. Lett. **99**, 062504 (2011).
[6] G. Catalan and J. F. Scott, Adv. Mater. **21**, 2463 (2009).
[7] M. Tonouchi, *35th International Conference on Infrared, Millimeter, and Terahertz Waves* (IEEE, Rome, 2010).
[8] D. S. Rana, L. Kawayama, K. Takahashi, and M. Tonouchi, Europhys. Lett. **84**, 67016 (2008).
[9] D. Talbayev, S. A. Trugman, Seongsu Lee, Hee Taek Yi, S.-W. Cheong, and A. J. Taylor, Phys. Rev. B **83**, 094403 (2011).
[10] M. P. Kostylev, A. A. Serga, T. Schneider, B. Leven, and B. Hillebrands, Appl. Phys. Lett. **87**, 153501 (2005).
[11] V. V. Kruglyak, S. O. Demokritov, and D. Grundler, J. Phys. D **43**, 264001 (2010).
[12] A. Khitun, M. Bao, and K. L. Wang, J. Phys. D **43**, 264005 (2010).
[13] R. Loudon, Adv. Phys. **17**, 243 (1968).
[14] P. A. Fleury and R. Loudon, Phys. Rev. **166**, 514 (1968).
[15] J. Nouet, D. J. Toms, and J. F. Scott, Phys. Rev. B **7**, 4874 (1973).
[16] S. Venugopalan, A. Petrou, R. R. Galazka, A. K. Ramdas, and S. Rodriguez, Phys. Rev. B **25**, 2681 (1982).
[17] M. I. Darby, Br. J. Appl. Phys. **18**, 1415 (1967).
[18] C. Kittel, *Introduction to Solid State Physics*, 8th ed. (Wiley, Hoboken, NJ, 2005), pp. 303–304.
[19] T. P. Devereaux and R. Hackl, Rev. Mod. Phys. **79**, 175 (2007).
[20] A. G. Gavriliuk, V. V. Struzhkin, L. S. Lyubutin *et al.*, JETP Lett. **86**, 197 (2007).
[21] A. G. Gavriliuk, L. S. Lyubutin, and V. V. Struzhkin, JETP Lett. **86**, 532 (2007).
[22] L. S. Lyubutin, A. G. Gavriliuk, and V. V. Struzhkin, JETP Lett. **88**, 524 (2008).
[23] A. G. Gavriliuk, V. Struzhkin, I. S. Lyubutin, I. A. Trojan, M. Y. Hu, and P. Chow, in *Materials Research at High Pressure*, edited by M. R. Manaa *et al.*, MRS Symposia Proceedings No. 987 (MRS, Warrendale, PA, 2007), pp. 147–152.
[24] M. Polomska, W. Kaczmare, and Z. Pajak, Phys. Status Solidi A **23**, 567 (1974).
[25] P. Fischer, M. Polomska, I. Sosnowska *et al.*, J. Phys. C **13**, 1931 (1980).
[26] X. Marti, P. Ferrer, J. Herrero-Albillos, J. Narvaez, V. Holy, N. Barrett, M. Alexe, and G. Catalan, Phys. Rev. Lett. **106**, 236101 (2011).